



Control of analyte electrolysis in electrospray ionization mass spectrometry using repetitively pulsed high voltage[☆]

Vilmos Kertesz, Gary J. Van Berkel^{*}

Organic and Biological Mass Spectrometry Group, Chemical Sciences Division, Oak Ridge National Laboratory, Oak Ridge, TN 37831-6131, United States

ARTICLE INFO

Article history:

Received 13 September 2010

Received in revised form 2 February 2011

Accepted 3 February 2011

Available online 21 February 2011

Keywords:

ESI-MS

Pulsed ESI

Analyte electrolysis control

Mass transport

Double layer relaxation

ABSTRACT

Analyte electrolysis using a repetitively pulsed high voltage ion source was investigated and compared to that using a regular, continuously operating direct current high voltage ion source in electrospray ionization mass spectrometry. The extent of analyte electrolysis was explored as a function of the length and frequency of the high voltage pulse using the model compound reserpine in positive ion mode. Using +5 kV as the maximum high voltage amplitude, reserpine was oxidized to its 2, 4, 6 and 8-electron oxidation products when direct current high voltage was employed. In contrast, when using a pulsed high voltage, oxidation of reserpine was eliminated by employing the appropriate high voltage pulse length and frequency. This effect was caused by inefficient mass transport of the analyte to the electrode surface during the duration of the high voltage pulse and the subsequent relaxation of the emitter electrode/electrolyte interface during the time period when the high voltage was turned off. This mode of ESI source operation allows for analyte electrolysis to be quickly and simply switched on or off electronically via a change in voltage pulse variables.

© 2011 Published by Elsevier B.V.

1. Introduction

The electrolysis inherent to the operation of the electrospray ionization (ESI) source used with mass spectrometry (MS) is a well known accompanying effect of generating unipolar spray droplets [1]. This reaction can substantially alter the analytes such that the ions observed in the gas phase have a different mass and/or charge than the species originally in the solution. For these reasons, gaining control over the electrolysis process is advantageous. Undesirable electrolysis of an analyte may be prevented by limiting the emitter electrode current [2] and/or the mass transport characteristics of the system [3,4], or by using an appropriate redox buffer [5–8]. “Planned” analyte electrolysis can be also very advantageous, providing the ability to create novel ionic species, probe analyte redox chemistry, and perform electrochemical ionization [9–16].

[☆] This manuscript has been authored by a contractor of the U.S. Government under Contract No. DE-AC05-00OR22725. Accordingly, the U.S. Government retains a paid-up, nonexclusive, irrevocable, worldwide license to publish or reproduce the published form of this contribution, prepare derivative works, distribute copies to the public, and perform publicly and display publicly, or allow others to do so, for U.S. Government purposes.

^{*} Corresponding author at: Chemical Sciences Division, Oak Ridge National Laboratory, 1 Bethel Valley Rd., Bldg. 4500S, Room S-140, Oak Ridge, TN 37831, United States. Tel.: +1 865 574 1922; fax: +1 865 576 8559.

E-mail address: vanberkelgj@ornl.gov (G.J. Van Berkel).

If the mass transport of the analyte to the electrospray emitter electrode is not limited, which is fundamental for full control over analyte electrolysis [1], the degree to which a particular analyte may be involved in direct electrolysis at this electrode is governed by the redox properties of the analyte and interfacial potential of the emitter electrode(s). Direct and precise control over interfacial potential of the emitter electrode is possible by using it as the working electrode in a three-electrode emitter system [17–20]. Incorporation of a potentiostat into the circuit also overcomes electrolysis current limitations imposed by the electrospray process. An incorporated potentiostat also provides new capabilities like electrochemical reduction of an analyte in positive ion mode and electrochemical oxidation of an analyte in negative ion mode [20]. However, with a specific goal to achieve complete electrolysis of the analyte of interest, for example, the potentiostat system provides an unnecessary precise control over the interfacial potential of the emitter electrode. Simple coarse control over this interfacial potential is possible by limiting the current available at the emitter electrode, which in turn indirectly controls the interfacial potential of the emitter electrode. Such control was accomplished by creating/disrupting an upstream current loop [21,22] or by changing the resistance in this current loop by changing the length of the connecting tubing between the emitter electrode and the upstream ground contact [2]. Controlling analyte electrolysis by changing the absolute value and the distribution of the available electrospray current between two emitter electrodes with different mass transport characteris-

tics using a battery-powered two-electrode emitter cell was also demonstrated [23]. However, as these methods are based on the control of the electrospray current, they are very much dependent on parameters that affect the electrospray current/electrode potential relationship (e.g., solution conductivity and applied electrospray voltage). These observations call for another approach that would provide a rapid control over the electrochemical reactions without the disadvantages of the methods described above.

In this paper, we conceptually present and demonstrate a new technique to either maximize or minimize the involvement of the electroactive analyte in the electrolysis process inherent to electrospray ionization. This technique utilizes rapid switching between the regular direct current (DC) electrospray high voltage and a pulsed high voltage, respectively. While other aspects of using a pulsed electrospray source have been investigated before (e.g., spray modes, spray stability, possibility to deposit fluid droplets onto surfaces, charged droplet generation, effect on mass spectrum, creating analyte and reagent ions for studying ion/ion reactions) [24–31], the effect on the electrolysis process compared to a continuous DC high voltage electrospray source has not previously been investigated. The emitter cell geometry and solution flow rate for the experiments described herein were chosen such that using the continuous DC electrospray source the mass transport of the analyte to the working electrode surface was efficient and the emitter electrode current magnitude was sufficient to effectively electrolyze the model analyte reserpine. The experimental results presented show that efficiency of analyte electrolysis depends on the length and frequency of the high voltage pulses, and that analyte electrolysis can be switched on and off simply by changing the voltage pulse variables. The ability to suppress analyte electrolysis is understood to be due to inefficient mass transport of the analyte to the electrode surface during the duration of the high voltage pulse and the subsequent relaxation of the emitter electrode/electrolyte interface during the time period when the high voltage is turned off.

2. Materials and methods

2.1. Samples and reagents

Reserpine (compound **1**, Aldrich, Milwaukee, WI) and dodecylethyldimethylammonium bromide (**2**, Aldrich) were obtained commercially and used without further purification. Solutions were prepared using acetonitrile (Burdick and Jackson, Muskegon, MI), water (Burdick and Jackson), ammonium acetate (99.999%, Aldrich) and acetic acid (PPB/Teflon grade, Aldrich).

2.2. ESI-MS setup

ESI-MS experiments were performed on an MDS Sciex API QSTAR Pulsar i time-of-flight mass spectrometer with a TurbolonSpray™ source (MDS Sciex, Concord, Ontario, Canada). Mass spectra were acquired with a porous flow through (PFT) electrode emitter spray assembly described in detail elsewhere [2]. The PFT electrode assembly was mounted in the TurbolonSpray™ source by simple exchange of the stainless steel bore-through union, nebulizer tube, and emitter capillary assembly that connects the solution flow into the source. The solution exited the electrode and was sprayed through a 3.5 cm length of 50 μm -i.d., 360 μm -o.d. fused silica capillary (70 nL volume) with a Taper Tip (New Objective, Inc.) held in place using appropriate ferrules and a nebulizer tube nut. Nebulizer gas (GAS 1) was set to 40 to appropriately nebulize the solution at the 10 $\mu\text{L}/\text{min}$ flow rate used in all experiments. To protect the PFT electrode emitter from plugging, a precolumn

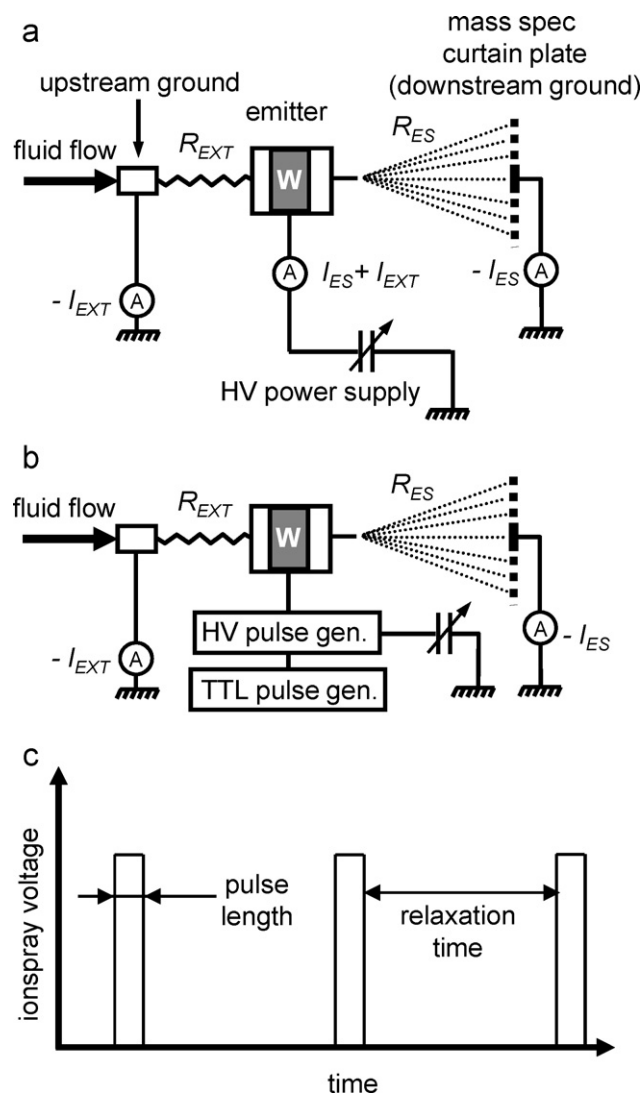
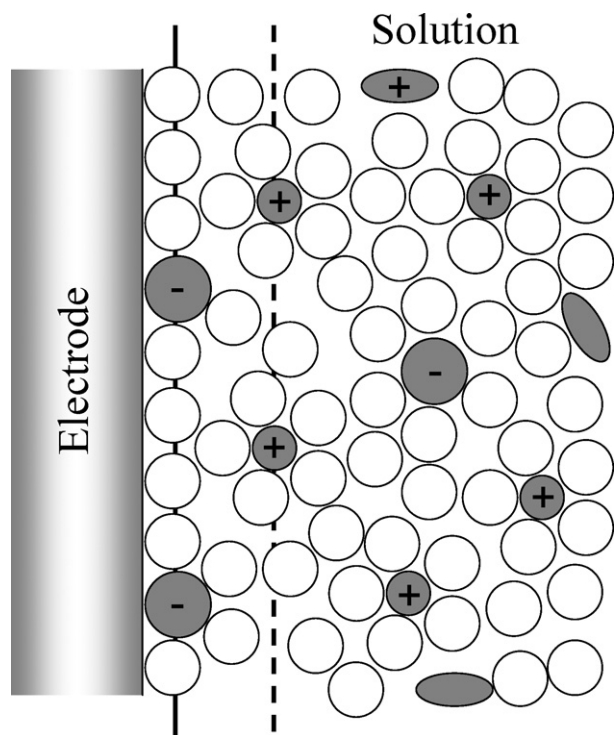


Fig. 1. (a) Diagram of the electrical circuit of the electrospray system shows the external current loop (with resistance R_{EXT} resulting in current I_{EXT}) between the upstream grounding point and the emitter, and the upstream electrospray circuit (with resistance R_{ES} resulting in current I_{ES}) between the emitter and the mass spectrometer as counter electrode. (b) Diagram of the pulsed voltage electrospray system. (c) Diagram of the potential program applied in the pulsed voltage electrospray system.

filter (0.5- μm porosity, Model 70-6570, ESA, Chelmsford, MA) was placed in the flow stream in all experiments.

Diagrams of the electrical circuits of the DC and the pulsed ESI sources are shown in Fig. 1a and b, respectively. In both cases, the circuit includes the external current loop (with resistance R_{EXT} resulting in current I_{EXT}) between the upstream grounding point and the emitter, and the upstream electrospray circuit (with resistance R_{ES} resulting in current I_{ES}) between the emitter and the mass spectrometer as counter electrode. Pulsed voltages in the circuit in Fig. 1b were generated by triggering a high voltage pulse generator (model PVX-4130, Directed Energy, Inc., Fort Collins, CO) supported by an external high voltage source (model 205B-05R, Bertain, Hicksville, NY) using a low-voltage TTL pulse generator (model DG 535, Stanford Res. Systems, Sunnyvale, CA). A modified ion source high voltage cable (P/N: 013596/E) fitted to the output of the high voltage pulse generator was used to transmit the high voltage pulses to the emitter. The low-voltage TTL pulse generator was used to adjust the length and frequency of the high voltage pulses, and these parameters in turn defined the time when



Scheme 1. Schematic illustration of the emitter electrode/electrolyte interface. Open circles, filled circles and ovals represent the solvent molecules, electrolyte ions and analytes, respectively.

ground potential was applied to the emitter electrode (relaxation time, Fig. 1c).

2.3. Safety

All electrical circuit components that float at the ESI high voltage should be handled with extreme care and preferably isolated from the user with appropriate shields and safety interlocks.

3. Results and discussion

3.1. Concept of controlled analyte electrolysis using pulsed high voltage ESI

The ability to control analyte electrolysis using pulsed high voltage utilizes the difference in analyte concentration between the ESI emitter electrode–electrolyte interface and the bulk phase. Scheme 1 illustrates the electrode/electrolyte interface including the double layer when no potential is applied on the electrode [32]. The inner Helmholtz layer (indicated left from the solid vertical line in Scheme 1) is built from a layer of solvent molecules and ions with specific adsorption. The outer, still rigid Helmholtz layer (indicated between the solid and the dashed vertical lines in Scheme 1) and the diffuse Gouy–Chapman layer (right from the dashed vertical line in Scheme 1) contain ions to counterbalance the charge in the inner Helmholtz layer (including charged/protonated analyte molecules, and neutral analyte molecules). The thickness of water layer (l_w) that is necessary to provide the Faradaic charge injected in a pulse (Q_F) can be calculated using Avogadro's number ($N_A = 6.023 \times 10^{23} \text{ mol}^{-1}$), the number of moles of electrons transferred during oxidation of one mol of water ($n=2$), the Faraday constant ($F = 9.648 \times 10^4 \text{ C mol}^{-1}$), the mean van der Waals diameter of water ($d_w = 0.282 \times 10^{-9} \text{ m}$) [33] and the real surface area of

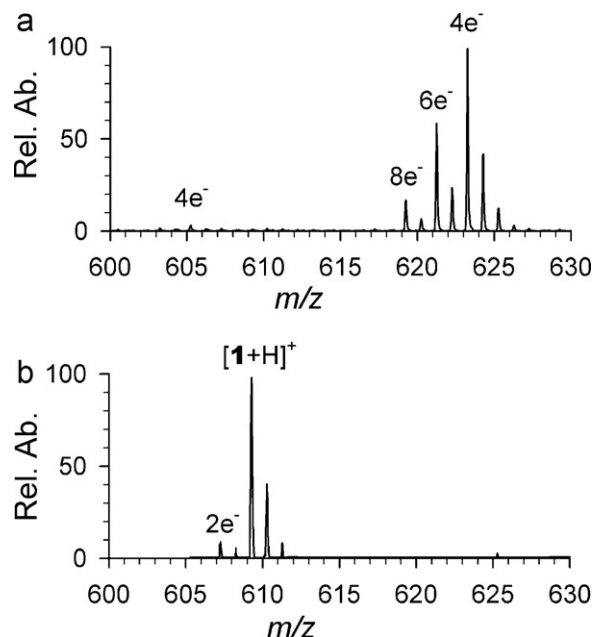


Fig. 2. Positive ion mode ESI mass spectra obtained for a 5 μM solution of compound 1 in 50/50/0.75 (v/v/v) water/acetonitrile/acetic acid, 5.0 mM ammonium acetate at a flow rate of 10 $\mu\text{L}/\text{min}$ using a PFT electrode with ionspray voltage of 5 kV applied (a) in DC mode and (b) as 100 Hz 10 μs pulses.

the PFT electrode used ($A = 170 \times 10^{-6} \text{ m}^2$) [2]:

$$l_w = \frac{Q_F N_A d_w^3}{nF A} \quad (1)$$

In the present setup the overall charge, including capacitive charges calculated from the current recorded during a pulse was 3.6 μC (not shown). If the entire charge is considered to be Faradaic (which overestimates the true l_w), we calculate that $l_w = 0.002 \times 10^{-9} \text{ m}$, which corresponds to about 1% of the monomolecular layer of water electrolyzed during a pulse. From this calculated distance and water layer percentage, one predicts that if an appropriate time is inserted between high voltage pulses sufficient to relax the double layer, the analyte should never reach the surface and only water molecules will be electrolyzed to supply the required current. In other words, if electrolysis is performed under appropriate repetitively pulsed high voltage conditions it should be possible to exclusively electrolyze the solvent that is proximal to the electrode surface.

3.2. Dependence of the extent of analyte electrolysis on pulse parameters

To further illustrate and support this concept, the extent of the electrolysis of our model compound reserpine (compound 1) using regular DC ESI (no relaxation time) was compared to the extent of electrolysis when using a pulsed high voltage setup that ensured ample time (approximately 10 ms which is in the upper range of the 1–10 ms relaxation time of the double layer for water [34]) to relax the double layer structure between high voltage pulses. Fig. 2a and b shows the positive ion mode ESI mass spectra of compound 1 obtained at a flow rate of 10 $\mu\text{L}/\text{min}$ with an ESI voltage of +5 kV applied using DC and pulsed high voltage (10 μs pulses with 100 Hz frequency), respectively. The use of regular DC high voltage resulted in extensive oxidation of reserpine producing the 4-, 6- and 8-electron oxidation products (see Scheme 2 and Fig. 2a). This behavior was expected based on our previous studies with the PFT electrode configuration [2]. In contrast, oxidation of reserpine was practically avoided using this specific pulsed high voltage function.

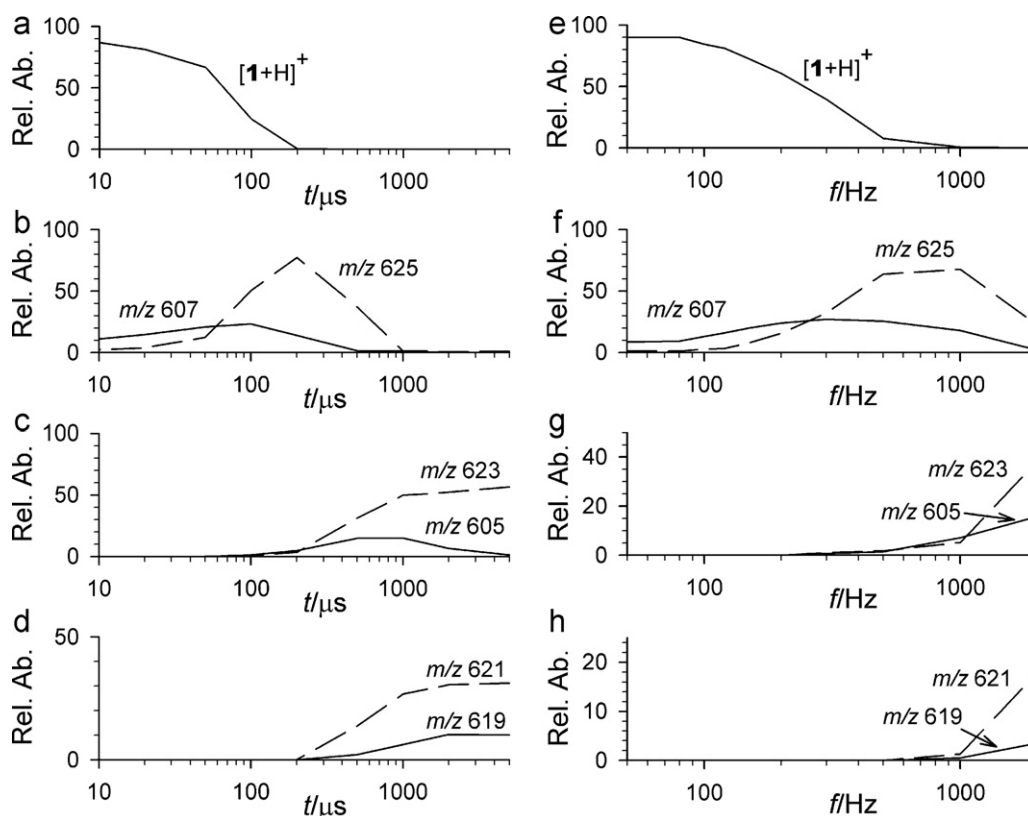
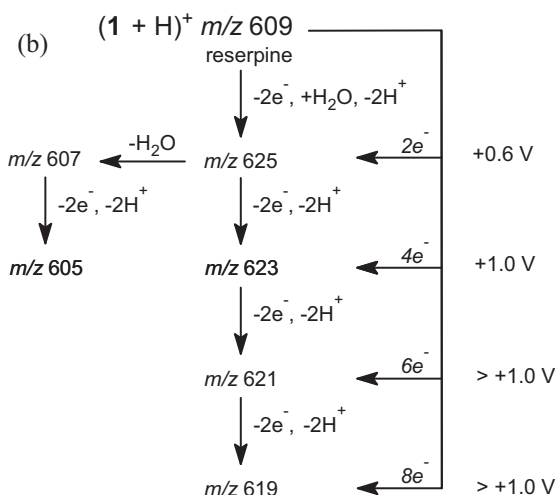
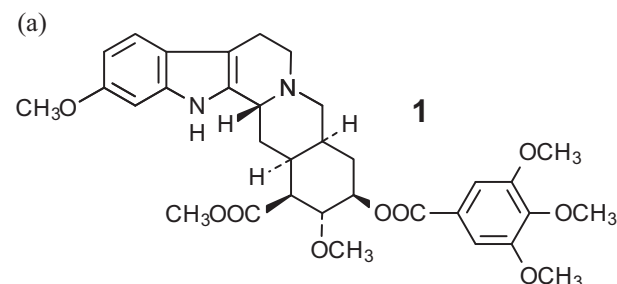


Fig. 3. Relative abundance of (a and e) compound **1** (m/z 609), (b and f) 2 e^- (m/z 607 and m/z 625), (c and g) 4 e^- (m/z 605 and m/z 623) and (d and h) 6 e^- (m/z 621) and 8 e^- (m/z 619) oxidation products of **1** as a function of pulse length using 5 kV pulses at a 100 Hz frequency and as a function of frequency using 50 μs -long 5 kV pulses, respectively. In all cases a 5 μM solution of **1** in 50/50/0.75 (v/v/v) water/acetonitrile/acetic acid, 5.0 mM ammonium acetate was sprayed at a flow rate of 10 $\mu\text{L}/\text{min}$ using a PFT electrode.



Scheme 2. (a) Reserpine (**1**) structure and (b) proposed oxidation pathways, ions observed and oxidation potentials.

A relative abundance of <10% of the 2-electron oxidation product dehydroreserpine observed at m/z 607 in the mass spectrum was the only indication that some reserpine oxidation might have still occurred. Note that m/z 607 is often observed in reserpine ESI mass spectra as a species at this mass is a product of aging of reserpine solutions [35,36].

The concept presented above predicts that by increasing the relaxation time between high voltage pulses the extent of analyte electrolysis will decrease. The relaxation time can be increased by either decreasing the frequency or decreasing the length of the high voltage pulse (Fig. 1c). Fig. 3a–d shows the dependence of the normalized percentages of reserpine and its 2-, the 4- and the 6- and 8-electron oxidation products, respectively, as a function of pulse length using 100 Hz pulse frequency. When pulse length was lower than approximately 50 μs , only a small amount of 2-electron oxidation product (Fig. 3b) was observed and compound **1** (Fig. 3a) was the base peak in the spectrum. When the pulse length was increased to 200 μs , compound **1** was no longer detected. In fact, a 2-electron oxidation product at m/z 625 was the base peak in the spectrum at this pulse length. Further increase in pulse length to 1 ms resulted in more effective reserpine oxidation indicated by the increasing relative abundances of the 4-, 6- and 8-electron oxidation products at m/z 605/623 (Fig. 3c), 621 and 619 (Fig. 3d), respectively. At the same time, the 2-electron oxidation product at m/z 625 practically disappeared from the mass spectrum. When the pulse length was increased beyond 1 ms, only a slight increase in the percentages of the 4-, 6- and 8-electron oxidation products at m/z 623, 621 and 619, respectively, was observed. The percentages of the 4-, 6- and 8-electron oxidation products at m/z 605/623, 621 and 619, respectively, at a pulse length of 2 ms (2.1/56.6, 31.2 and 10.1%, respectively) were comparable to those percentages obtained

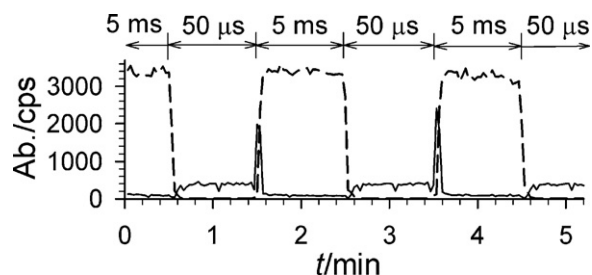


Fig. 4. Absolute abundance of (solid line) compound **1** (m/z 609) and (dashed line) $2 e^-$ (m/z 625) oxidation product of **1** as a function of time using 5 ms and 50 μ s-long 5 kV pulses at a 100 Hz frequency, as indicated, when a 5 μ M solution of **1** in 50/50/0.75 (v/v/v) water/acetonitrile/acetic acid, 5.0 mM ammonium acetate was sprayed at a flow rate of 10 μ L/min using a PFT electrode.

using DC high voltage (3.4/56.7, 31.0 and 8.9%, respectively, see Fig. 2a).

Pulse frequency dependence, over the range of 50–2000 Hz, of the relative intensities of the reserpine-related species at a fixed 50 μ s pulse length was also investigated using the same solution (Fig. 3e–h). The pulse length was selected based on the results shown in Fig. 3a–d. In those experiments the use of this pulse length and 100 Hz resulted in only minor analyte oxidation. If our proposed mechanistic concept is correct then increasing the pulse frequency (i.e., shorter relaxation time) would be expected to result in increased analyte oxidation. In fact, compound **1** (Fig. 3e) dominated the mass spectrum when the pulse frequency was lower than approximately 100 Hz. Increasing the pulse frequency to between 500 and 1000 Hz resulted in the 2-electron oxidation product at m/z 625 being the base peak in the mass spectrum (Fig. 3f). Further increase in pulse frequency to 2000 Hz resulted in an even more effective reserpine oxidation indicated by the dominance of the 4- and 6-electron oxidation products at m/z 623 (Fig. 3g) and 621 (Fig. 3h) in the mass spectrum, respectively, coupled to a decreased amount of the 2-electron oxidation product at m/z 625.

The data in Fig. 3 showed that either decreasing the pulse length at a fixed pulse frequency or decreasing the pulse frequency at a fixed pulse length both decrease the extent of analyte electrolysis. Changing these parameters can be accomplished rapidly via electronic control, which in turn should immediately affect the extent of analyte electrolysis observed. Fig. 4 shows the time transients of the absolute abundances of reserpine (solid line) and its 2-electron oxidation product at m/z 625 (dashed line) when switching between 5 ms and 50 μ s-long, 100 Hz frequency +5 kV pulses on the emitter electrode at 60 s intervals. As expected and observed previously, these data show that the longer pulse length (shorter relaxation time) resulted in complete reserpine oxidation, while the use of shorter pulses prevented analyte oxidation. However the expected rapid change in analyte electrolysis when switching between the two states of operation actually took approximately 4–6 s to observe. This time delay did not correspond well with the calculated flush time of the cell. Simple replacement of the approximately 170 nL total volume of the electrode assembly including 100 nL nominal swept and 70 nL spray capillary volumes would have taken about 1 s to complete at the 10 μ L/min flow rate applied [2]. This result suggests that the washout efficiency of the electrode assembly will be a major factor for actual analytically useful switching speed to turn on and off analyte electrolysis. One also notes a short-lived, but significant mass spectral signal increase for compound **1** at the beginning of the application of the 5 ms pulses. We attribute this behavior to the effect of increased percentage of time the high voltage was turned on during this washout period resulting in higher absolute signal for compound **1** for the reasons discussed in detail below.

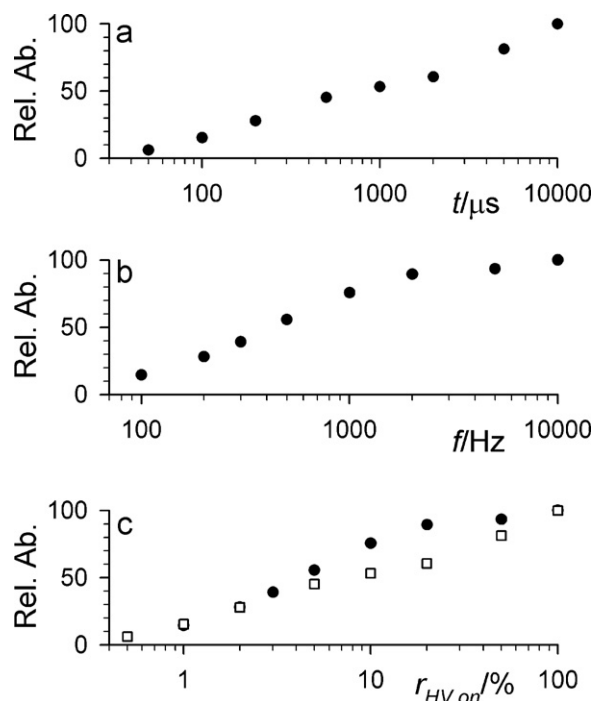


Fig. 5. Relative abundance of compound **2** as function of (a) pulse length using 5 kV pulses at a 100 Hz frequency, (b) frequency using 100- μ s-long 5 kV pulses and (c) time percentage while the high voltage was applied calculated from the pulse width and frequency from figures (□) (a) and (●) (b). In all cases a 0.1 μ M solution of **2** in 50/50/0.75 (v/v/v) water/acetonitrile/acetic acid, 5.0 mM ammonium acetate was sprayed at a flow rate of 10 μ L/min using a PFT electrode.

3.3. Dependence of the absolute mass spectral signal on pulse parameters

The results presented above demonstrated that altering electronically the length and/or frequency of the high voltage pulses provided a means to control the extent of analyte electrolysis at the electrospray emitter electrode. However, when operating to minimize analyte electrolysis by a decrease of either the frequency or the length of the high voltage pulse, the absolute mass spectral signal intensity for the analyte derived ions was observed to decline. To examine this effect, free from artifacts due to analyte electrolysis, the non-electroactive, preformed ion dodecylethyltrimethylammonium (compound **2**) was used as test analyte for this study. Fig. 5a and b shows the dependence of the mass spectral signal level of a 0.1 μ M solution of compound **2** (observed at m/z 242) as function of pulse length using a 100 Hz pulse frequency and as a function of pulse frequency using 100 μ s pulse length, respectively. Note that the highest signal levels measured correspond to a DC ESI situation (no relaxation time between pulses). Overall, the mass spectral signal gradually increased with increasing pulse length and pulse frequency. This observation is in agreement with previous reports on pulsed ESI [24,28,29]. Gas phase ions were observed when the high voltage was turned on but there were no detectable ions when the spray was turned off. Thus, pulsed high voltage ESI necessarily presents a total ion signal that is an average (which varies with pulse parameters) of the signal observed during a continuous spray using DC high voltage and the zero signal observed in the absence of high voltage.

To more quantitatively evaluate this relationship, the mass spectral signal observed was plotted in Fig. 5c as the percentage of time the high voltage was turned on as calculated from both Fig. 5a and b. Two unexpected anomalies are apparent in this plot. First, the mass spectral signal was not linearly correlated to the percentage of time the high voltage was turned on (note that Fig. 5c is a

semi-logarithmic plot). Even when high voltage was turned on for only 1% or 10% of the total time ($r_{HV\ on} = 1\%$ and $r_{HV\ on} = 10\%$, respectively), the mass spectral signal was 15% or 55–75% of that of the maximum signal observed in DC ESI ($r_{HV\ on} = 100\%$), respectively. The exact cause of this non-linearity is not known. The second unexpected anomaly in Fig. 5c was the hysteresis between plots created using fixed pulse length (filled symbols) and fixed pulse frequency (open symbols). Higher mass spectral signal observed in the $5\% \leq r_{HV\ on} \leq 50\%$ range using fixed 100 μs pulse length over using a fixed 100 Hz frequency indicated that a larger number of shorter pulses created more ions for mass spectral analysis than fewer, but longer pulses.

The dependence of mass spectral signal on $r_{HV\ on}$ shown in Fig. 5c for compound **2** was briefly compared to that for reserpine (compound **1**). According to Figs. 2 and 3, oxidation of reserpine was maximized using DC ESI and was minimized using pulsed high voltage ESI with a pulse frequency of 100 Hz and a pulse length of 50 μs . These pulsed high voltage ESI parameters correspond to $r_{HV\ on} = 0.5\%$ for which data in Fig. 5 suggests an MS signal intensity of approximately 6% of that expected when using DC ESI. In fact, the absolute intensity of compound **1** at m/z 609 measured using a pulse frequency of 100 Hz and a pulse length of 50 μs was approximately 7% of the sum of that of m/z 623, 621 and 619 obtained using DC ESI. This close match between data obtained from two independent measurements, despite the possible differing ionization efficiencies of reserpine and its oxidation products, confirms that data in Fig. 5 can be successfully applied to predict MS signal intensity changes when switching from DC ESI to pulsed high voltage ESI.

This observed decline in absolute mass spectral signal under the pulsed high voltage ESI conditions that prevent analyte electrolysis could negatively affect the sensitivity of an ESI-MS analysis. However, on the basis of our understanding of the effect, there do appear to be ways to mitigate the issue. One possible solution would be a multi-electrode emitter system in which high voltage is coupled sequentially to the electrodes such that the pulse length and pulse frequency on the electrodes would ensure that the analyte of interest cannot be oxidized at any of the individual electrodes. The double layer on any one electrode would be provided sufficient relaxation time to avoid analyte electrolysis while other electrodes in the array to which high voltage is still applied would provide the required electrospray current for the system. For example, presented with an emitter system with 20 individual electrodes to which a pulse frequency of 100 Hz and a pulse length of 50 μs ($r_{HV\ on} = 10\%$) were applied to the electrodes in a sequence would be predicted to provide approximately 55–75% of the maximum signal observed in DC ESI, based on Fig. 5.

4. Conclusion

In this paper, we have presented a new simple electronic means to control the extent of analyte electrolysis in ESI-MS. This method utilized a pulsed high voltage ESI source in which a simple change in the applied pulse length and/or pulse frequency was used to alter the extent of analyte electrolysis. The ability to suppress analyte electrolysis with the pulsed high voltage ESI source described here is a result of inefficient mass transport of the analyte to the electrode surface during the duration of the high voltage pulse and the subsequent relaxation of the emitter electrode/electrolyte interface during the time period when the high voltage is turned off. The model compound reserpine was completely oxidized to a mixture of its 4-, 6- and 8-electron oxidation products using a pulse frequency of 100 Hz and a pulse length of 2000 μs . In contrast, oxidation of reserpine was prevented by employing the same 100 Hz pulse frequency but with a pulse length of 50 μs . These lower pulse

frequencies and/or shorter pulse lengths that avoided analyte electrolysis do result in an overall drop in the mass spectral signal by about 90% in the present system. However, it should be possible in the future to overcome this issue with an appropriately configured system, such as an emitter electrode.

In general, the technique presented here opens the door to the possibility of a simple tunable (nano)ESI source that can be electronically switched rapidly between on and off modes of analyte electrolysis. This provides the capability, for example, to obtain data with analyte electrolysis on and off for rapid temporal changes in analyte concentration as in an eluting chromatographic peak to achieve maximum ionization/sensitivity and/or to obtain more detailed chemical information (e.g., redox properties).

Acknowledgments

ESI-MS instrumentation and the PFT cell were provided through a Cooperative Research and Development Agreement with MDS SCIEX and ESA Biosciences, Inc. (CRADA No. ORNL02-0662), respectively. This work was supported by the Division of Chemical Sciences, Geosciences, and Biosciences, Office of Basic Energy Sciences, United States Department of Energy under Contract DE-AC05-00OR22725 with ORNL, managed and operated by UT-Battelle, LLC.

References

- [1] G.J. Van Berkel, V. Kertesz, *Anal. Chem.* 79 (2007) 5510.
- [2] G.J. Van Berkel, V. Kertesz, M.J. Ford, M.C. Granger, *J. Am. Soc. Mass Spectrom.* 15 (2004) 1755.
- [3] V. Kertesz, G.J. Van Berkel, *J. Mass Spectrom.* 36 (2001) 204.
- [4] G.J. Van Berkel, K.G. Asano, V. Kertesz, *Anal. Chem.* 74 (2002) 5047.
- [5] A.J. Bard, L.R. Faulkner, *Electrochemical Methods*, John Wiley, New York, 2001.
- [6] M. Moini, P. Cao, A.J. Bard, *Anal. Chem.* 71 (1999) 1658.
- [7] E. Peintler-Krivan, G.J. Van Berkel, V. Kertesz, *Rapid Commun. Mass Spectrom.* 24 (2010) 1327.
- [8] E. Peintler-Krivan, G.J. Van Berkel, V. Kertesz, *Rapid Commun. Mass Spectrom.* 24 (2010) 3368.
- [9] G.J. Van Berkel, S.A. McLuckey, G.L. Glish, *Anal. Chem.* 64 (1992) 1586.
- [10] X.X. Xu, S.P. Nolan, R.B. Cole, *Anal. Chem.* 66 (1994) 119.
- [11] T. Guaratini, R. Vessecchi, E. Pinto, P. Colepiccolo, N.P. Lopes, *J. Mass Spectrom.* 40 (2005) 963.
- [12] T.T. Guaratini, R.L. Vessecchi, F.C. Lavarda, P.M.B.G.M. Campos, Z. Naal, P.J. Gates, N.P. Lopes, *Analyst* 129 (2004) 1223.
- [13] G.J. Van Berkel, J.M.E. Quirke, A. Dilley, R. Tigani, T.R. Covey, *Anal. Chem.* 70 (1998) 1544.
- [14] D. Rondeau, D. Kreher, M. Cariou, P. Hudhomme, A. Gorgues, P. Richomme, *Rapid Commun. Mass Spectrom.* 15 (2001) 1708.
- [15] A. Dupont, J.-P. Gisselbrecht, E. Leize, L. Wagner, A. Van Dorsselaer, *Tetrahedron Lett.* 35 (1994) 6083.
- [16] K. Hiraoka, K. Aizawa, K. Murata, S. Fujimaki, *J. Mass Spectrom. Soc. Jpn.* 43 (1995) 77.
- [17] X. Xu, W. Lu, R.B. Cole, *Anal. Chem.* 68 (1996) 4244.
- [18] W. Lu, X. Xu, R.B. Cole, *Anal. Chem.* 69 (1997) 2478.
- [19] G.J. Van Berkel, K.G. Asano, M.C. Granger, *Anal. Chem.* 76 (2004) 1493.
- [20] V. Kertesz, G.J. Van Berkel, M.C. Granger, *Anal. Chem.* 77 (2005) 4366.
- [21] L.L. Konermann, E.A. Silva, O.F. Sogbein, *Anal. Chem.* 73 (2001) 4836.
- [22] R.A. Ochran, L.J. Konermann, *Am. Soc. Mass Spectrom.* 15 (2004) 1748.
- [23] V. Kertesz, G.J. Van Berkel, *J. Am. Soc. Mass Spectrom.* 17 (2006) 953.
- [24] S.B. Sample, R. Bollini, *J. Colloid Interf. Sci.* 41 (1972) 185.
- [25] M.D. Paine, M.S. Alexander, K.L. Smith, M. Wang, J.P.W. Stark, *Aer. Sci.* 38 (2007) 315.
- [26] S.B.Q. Tran, D. Byun, V.D. Nguyen, T.S. Kang, *Phys. Rev. E* 80 (2009) 026318.
- [27] Y. Lu, F. Zhou, W.Q. Shui, L.P. Bian, P.Y. Yang, *Anal. Chem.* 73 (2001) 4748.
- [28] J.F. Wei, W.Q. Shui, F. Zhou, Y. Lu, K.K. Chen, G.B. Xu, P.Y. Yang, *Mass Spectrom. Rev.* 21 (2002) 148.
- [29] W.T. Berggren, M.S. Westphall, L.M. Smith, *Anal. Chem.* 74 (2002) 3443.
- [30] B.F. Chao, C.J. Chen, F.A. Li, G.R. Her, *Electrophoresis* 27 (2006) 2083.
- [31] X. Liang, Y. Xia, S.A. McLuckey, *Anal. Chem.* 78 (2006) 3208.
- [32] J.O'M. Bockris, M.A.V. Devanathan, K. Muller, *Proc. R. Lond. Soc. Ser. A: Mater. Phys. Sci.* 274 (1963) 55.
- [33] F. Franks, *Water: A Matrix of Life*, second ed., Royal Society of Chemistry, Cambridge, 2000.
- [34] O. Teschke, E.F. de Souza, G. Ceotto, *Langmuir* 15 (1999) 4935.
- [35] G.E. Wright, T.Y. Tang, *J. Pharm. Sci.* 81 (1972) 299.
- [36] S.P. Singh, V.I. Stenberg, S.S. Parmar, *Chem. Rev.* 80 (1980) 269.